Technische Universität München
Lehrstuhl für Nachrichtentechnik
Prof. Dr.sc.tech. Gerhard Kramer

Research Internship

Geometric and Probabilistic Constellation Shaping with Autoencoders

Vorgelegt von:
David de Andrés Hernández

München, October 2022

Betreut von:
M.Sc. Francesca Diedolo

Research Internship am
Lehrstuhl für Nachrichtentechnik (LNT)
der Technischen Universität München (TUM)
Titel : Geometric and Probabilistic Constellation Shaping with Autoencoders
Autor : David de Andrés Hernández

David de Andrés Hernández
Boschetsriederstr. 55A
81379 München
deandres.hernandez@tum.de

Ich versichere hiermit wahrheitsgemäß, die Arbeit bis auf die dem Aufgabensteller bereits bekannte Hilfe selbständig angefertigt, alle benutzten Hilfsmittel vollständig und genau angegeben und alles kenntlich gemacht zu haben, was aus Arbeiten anderer unverändert oder mit Abänderung entnommen wurde.

München, 26.10.2022

Ort, Datum (David de Andrés Hernández)

Contents

Abstract **1**

1 Introduction **3**

2 Preliminaries **5**
2.1 Probabilistic Constellation Shaping 5
2.1.1 Introduction 5
2.1.2 Capacity Gap for Uniform Continuous Input 7
2.1.3 Uniform Discrete Input Bound 9
2.1.4 Capacity-achieving distributions 10
2.2 Autoencoders 12
2.2.1 Feed-Forward Neural Networks 12
2.2.2 Stochastic Gradient Descent 13
2.2.3 Autoencoders 13
2.3 Outlook 14

3 Contribution **15**
3.1 Notation 15
3.2 First implementation 15
3.2.1 Optimization of trainable parameters 15
3.2.2 Autoencoder Architecture 17
3.2.3 Autoencoder Performance 18
3.3 Second implementation 21
3.3.1 Optimization of trainable parameters 21
3.3.2 Autoencoder Architecture 24
3.3.3 Autoencoder Performance 24

4 Conclusions **27**

List of Abbreviations **29**

Bibliography **31**

Abstract

Finding sets of optimal parameters for communication systems with complex or unknown channel models is a problem which can be approached thanks to machine learning (ML). These parameters refer to the location and probability of occurrence of the constellation points. Together with autoencoders, pioneered in [OH17], which optimize jointly transmitter and receiver; and the appropriate loss function, which must maximize the channel's mutual information, this ML-based method has shown close-to-optimal results in [SAAH19] and [AC21] when performed over the additive white gaussian noise (AWGN) channel. Yet, one particular challenge of this approach is learning a categorical distribution using a stochastic neural network, as backpropagating through the samples requires dealing with non-differentiable layers. In other words, learning a discrete probability distribution for the symbols occurrence requires that the sampling mechanism is differentiable, so that the gradient of the loss w.r.t the probability distribution can be computed via backpropagation. While the method proposed by Stark *et al.* leverages the Gumbel-Softmax gradient estimator [JGP16], Aref and Chagnon suggest an ad-hoc correction of this gradient after backpropagation. In this work, we break-down and analyze the benefits and drawbacks of each approach to further understand their potential and applicability over more complex channels.

1 Introduction

The constant demand for higher capacity digital links has motivated the development of communication schemes which approach closer and closer the analytical limit of the channel capacity. According to the definition of channel capacity, sending a single bit per time-frequency slot is inefficient. For this reason, higher-order modulations like amplitude shift keying (ASK) or quadrature amplitude modulation (QAM) are used for better efficiency. Under these modulation schemes, the receiver handles more than two signal points per real dimension — the set of spacial signal points is known as constellation. However, these schemes present a constant-width gap to the capacity limit. This is due to the use of both uniform and discrete probability distributions for the occurrence of the constellation points. While it is not possible to move away from the discrete distributions because of the digital nature of the communication, constellations with specific non-uniform distributions and optimized spatial locations can lead to further capacity improvements.

Constellation shaping thus, is a technique which seeks to optimize the distribution of the transmit symbols. Furthermore, this optimization unfolds into the improvement of the constellation points' location, their occurrence probability or both simultaneously. The first is known as geometric shaping while the latter is known as probabilistic shaping. In both cases, the goal is to maximize the mutual information (MI) of the channel input X and output Y, which we denote with $I(X;Y)$, by optimizing the constellation. This optimization problem arises from the definition of channel capacity C:

$$C = \max_{p(X)} I(X;Y). \tag{1.1}$$

Currently, the optimal $p(x)$ has only been found for specific channels, such as the AWGN, since knowledge of the channel distribution $p(y|x)$ is required. Still, solving (1.1) can become mathematically intractable despite knowing $p(y|x)$.

Here is where the use of machine-learning is key for finding constellations which maximize $I(X;Y)$, without analytical knowledge of the channel or with very complex $p(y|x)$. As shown in [OH17], the complete communication system can be interpreted as an autoencoder. This approach tackles the physical layer by optimizing the end-to-end per-

formance instead of the performance of the individual components. To achieve this, the loss function, against which the trainable parameters will be optimized, must be carefully selected. What is more, geometric shaping under the autoencoder framework has been already performed in [OH17] and [JEY+18]. Still, learning a probability distribution presents an additional challenge — the sampling mechanism must be differentiable. On the contrary, if the sampling mechanism is not differentiable, the numerical approximations for computing the gradient of the trainable parameters become imprecise due to the change of statistics in the training set. [SAAH19] and [AC21] address this problem with different proposals. Their results show that joint probabilistic and geometric shaping outperform the PS-QAM scheme from [BSS15] and approach the limit to within 0.1 dB in the AWGN channel. Nonetheless, the existence of multiple and apparently different architectures invites for a comparative study. Consequently, in this work we implement and discuss the architectures proposed by [SAAH19] and [AC21].

The rest of this document is organized as follows. Chapter 2, Preliminaries, presents the fundamentals of classical Probabilistic constellation systems as well as of autoencoder systems. Chapter 3, Contribution, presents a comparative study of two autoencoder architectures which can perform joint probabilistic and geometric constellation shaping and highlights their limitations. Chapter, Conclusions, 4 wraps-up this work.

2 Preliminaries

2.1 Probabilistic Constellation Shaping

In this section our goal is to present the capacity limitations of the commonly used ASK and QAM modulation schemes. These schemes are penalized for two reasons:

1. They use uniform probability densities.
2. The constellation points are equidistant.

In the following we explain the nature of these penalties.

2.1.1 Introduction

We begin with an important result from Information theory. Under a second-moment constraint, also known as power constraint, the probability distribution which maximizes the differential entropy is the Gaussian distribution, denoted with p_G. We thus have

$$h(X) \leq \frac{1}{2} \log \left(2\pi e \sigma^2\right) \tag{2.1}$$

where $\sigma^2 = \mathbb{E}[X^2]$, and with equality if and only if X is Gaussian-distributed. More generally in the multi-dimensional case we have

$$h(\underline{X}) \leq \frac{1}{2} \log \left((2\pi e)^n |\mathbf{Q}_{\underline{X}}|\right) \tag{2.2}$$

where we have considered a random column vector $\underline{X}$ of dimension n, mean $\mathbb{E}[\underline{X}] = \underline{m}$ and covariance matrix

$$\mathbf{Q}_{\underline{X}} = \mathbb{E}[(\underline{X} - \underline{m})(\underline{X} - \underline{m})^\intercal] \tag{2.3}$$

and equality in (2.2) if only if the elements of $\underline{X}$ are jointly Gaussian.

Lets now consider an AWGN channel with Gaussian input X, of zero mean and variance P; Gaussian noise Z, of zero mean and variance N; and output Y; i.e. $Y = X + Z$.

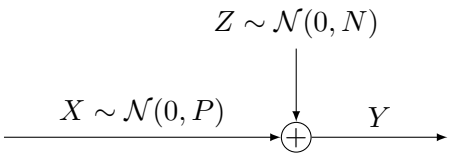

Furthermore, the capacity of the AWGN is

$$\begin{aligned} C(P) &= \max_{P_X : \mathbb{E}[X^2] \leq P} \mathbb{I}(X;Y) && (2.4)\\ &= \max_{P_X : \mathbb{E}[X^2] \leq P} [h(Y) - h(Y|X)] && (2.5)\\ &= \frac{1}{2}\log(2\pi e(P+N)) - \frac{1}{2}\log(2\pi eN) && (2.6)\\ &= \frac{1}{2}\log\left(1 + \frac{P}{N}\right). && (2.7) \end{aligned}$$

We can express the mutual information

$$\mathbb{I}(X;Y) = h(Y) - h(Y|X) \tag{2.8}$$

in two parts, the differential entropy of the output and the conditional differential entropy of the output given the input. We expand the second term as

$$\begin{aligned} h(Y|X) &= h(Y - X|X) && (2.9)\\ &= h(Z|X) && (2.10)\\ &= h(Z) = \frac{1}{2}\log\left(2\pi e\sigma^2\right) && (2.11) \end{aligned}$$

and observe that the term $h(Y|X)$ does not depend on how X is distributed. In contrast, $h(Y)$ does depend on how X is distributed by

$$p_Y(y) = \int_{-\infty}^{\infty} p_X(X) p_Z(y - x)\, dx = (p_X \star p_Z)(y). \tag{2.12}$$

To circumvent the fact that it is difficult to find a closed-form expression of $h(Y)$, we make use of the information divergence as

$$h(Y) \overset{(a)}{=} h(Y_G) - \mathbb{D}(p_Y \| p_G) \tag{2.13}$$

where (a) arises from the fact that $\mathbb{X}(p_X \| p_G) = h(Y_G)$ if and only if p_X has zero mean and variance P as p_G. (2.13) is very useful as it allows us to express the differential entropy of the output in terms of the information divergence between p_G and any other

distribution by means of the cross entropy.
Now we can rewrite 2.8 as

$$\begin{aligned}
\mathbb{I}(X;Y) &= h(Y) - h(Y|X) && (2.14)\\
&= h(Y) - h(Z) && (2.15)\\
&= h(Y_G) - \mathbb{D}(p_Y \| p_G) - h(Z) && (2.16)\\
&= [h(Y_G) - h(Z)] - \mathbb{D}(p_Y \| p_G) && (2.17)\\
&= C(P/\sigma^2) - \mathbb{D}(p_Y \| p_G). && (2.18)
\end{aligned}$$

This last result indicates that the loss of MI when using a distribution P_X different than P_G is the informational divergence $\mathbb{D}(p_Y \| p_G)$. In other words, if the Gaussian distribution is not used, the capacity penalty is characterized by $\mathbb{D}(p_Y \| p_G)$.

2.1.2 Capacity Gap for Uniform Continuous Input

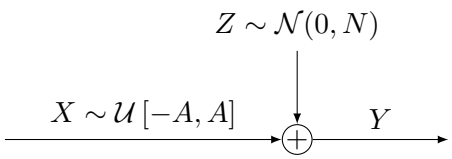

We would like now to understand how far a uniform distribution is from (2.1). To do this, we will follow the approach presented in [Bö18] to lower bound the MI. Start by defining X_u as a uniformly distributed input on the interval $[-A, A]$ where A is carefully chosen so that $\mathbb{E}[{X_u}^2] = P$. The corresponding output is Y_u and we proceed

$$\begin{aligned}
\mathbb{I}(X_u;Y_u) &= C(\text{snr}) - \mathbb{D}(p_{Y_u} \| p_{Y_G}) && (2.19)\\
&\geq C(\text{snr}) - \mathbb{D}(p_{X_u} \| p_{X_G}) && (2.20)\\
&= C(\text{snr}) - [h(X_G) - h(X_u)] && (2.21)\\
&= C(\text{snr}) - \frac{1}{2}\log_2\left(\frac{\pi e}{6}\right). && (2.22)
\end{aligned}$$

In Figure 2.1 we display the derived lower bound and observe that the capacity loss, originated from the use of a uniform input density, is never more than $\frac{1}{2}\log_2\frac{\pi e}{6}$ independent of the signal-to-noise ratio (SNR). To show that the shaping gap is tight, it is necessary to proof an upper bound for $\mathbb{I}(X_u;Y_u)$ that approaches 2.22 with increasing SNR. We refer the reader to [Bö18], Section 4.3, for this proof.

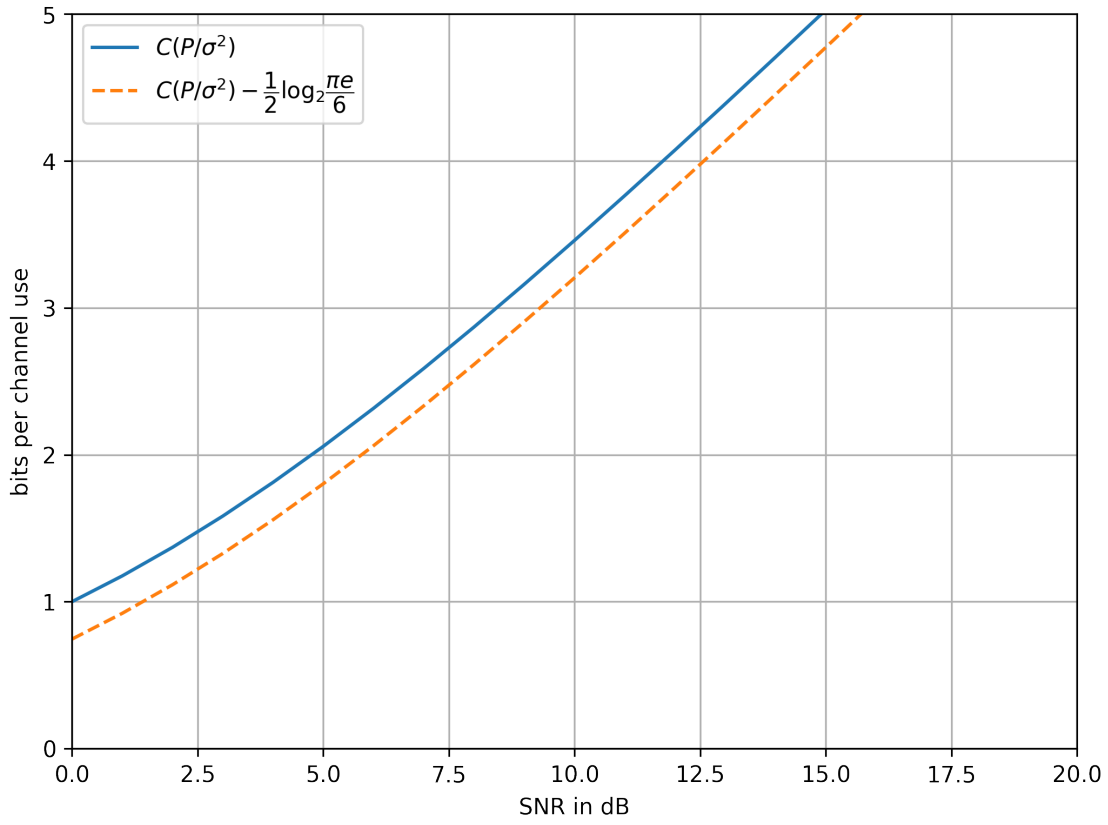

Figure 2.1: AWGN channel capacity gap. The orange line indicates the upper capacity bound for any uniformly distributed constellation.

2.1.3 Uniform Discrete Input Bound

We now show the penalty received for the use of an equidistant M-ASK constellation. We define the constellation points as

$$\mathcal{X} = \{\pm\Delta 1, \pm\Delta 3, \ldots, \Delta(M-1)\}, \tag{2.23}$$

where Δ is the scaling factor of the constellation, so that the channel input is X. If X_M is uniformly distributed, the resulting power is

$$P = \mathbb{E}\left[X_M^2\right] = \Delta^2 \frac{M^2-1}{3}. \tag{2.24}$$

Theorem 1 (Uniform Discrete Input Bound)**.** *The mutual information achieved by X_M is lowered bounded by*

$$\mathbb{I}(X_M;Y_M) \geq \frac{1}{2}\log_2\left(\frac{M^2}{M^2-1}\right) - \frac{1}{2}\log_2\left[2\pi e\left(\frac{P}{M^2-1}+\frac{P}{1+P/\sigma^2}\right)\right] \tag{2.25}$$

$$< C(snr) - \frac{1}{2}\log_2\left(\frac{\pi e}{6}\right) - \frac{1}{2}\log_2\left[1+\left(\frac{2^{C(snr)}}{M}\right)^2\right] \tag{2.26}$$

$$< C(snr) - Penalty(Uniform\ dist.) - Penalty(Equidistant\ dist.) \tag{2.27}$$

where $snr = P/\sigma^2$.

We refer the reader to [Bö18], section 4.5, for the proof. Theorem 1 shows our goal, namely that both the usage of a uniform distribution and an equidistant constellation penalizes the capacity. We can additionally compute the relation between the constellation size, M, and $C(\text{snr})$ so that the resulting MI is within a constant gap of capacity. To make this result even more attractive, we increase the constraint for the gap to match the order of the distribution loss (0.255 bits). We obtain

$$-\frac{1}{2}\log_2\left[1+\left(\frac{2^{C(\text{snr})}}{M}\right)^2\right] \leq -\frac{\log_2 e}{2}\left(\frac{2^{C(\text{snr})}}{M}\right)^2 = \frac{1}{4} \tag{2.28}$$

$$\Leftrightarrow M = 2^{C(\text{snr})+\frac{1}{2}+\frac{1}{2}\log_2\log_2 e} \tag{2.29}$$

by using $\log_e(x) \leq (1-x)$. So if

$$\log_2 M \approx C(\text{snr}) + 0.77, \tag{2.30}$$

then the mutual information is within 0.5 bit of capacity.

2.1.4 Capacity-achieving distributions

We now address the question of finding the discrete probability distribution which maximizes the capacity. Such distribution should be free of the $\frac{1}{2}\log_2\left(\frac{\pi e}{6}\right)$ penalty. We use again an ASK constellation with M signal points (in practice, M is a power of 2) given by

$$\mathcal{X} = \{\pm 1, \pm 3, \ldots, (M-1)\}. \tag{2.31}$$

Let X be a random variable with distribution P_X over $\mathcal{X}$. As before, we scale X by a $\Delta > 0$ and the resulting input/output relation for an AWGN channel becomes

$$Y = \Delta X + Z \tag{2.32}$$

In consequence, the MI of the channel input and output is

$$\begin{aligned} \mathbb{I}(\Delta X; Y) &= \mathbb{I}(\Delta X; \Delta X + Z) && (2.33)\\ &= \mathbb{I}(\Delta X; \Delta X + Z) && (2.34) \end{aligned}$$

where the second equality follows because (ΔX) is a deterministic function of X and vice-versa. Under an input average power constraint P, the scaling Δ and the distribution P_X must be chosen to satisfy

$$\mathbb{E}[(\Delta X)^2] \leq P. \tag{2.35}$$

Formally, our optimization problem is the following

$$C(P/\sigma^2) = \max_{\Delta, P_X : \mathbb{E}[(\Delta X)^2] \leq P} \mathbb{I}(X; \Delta X + Z). \tag{2.36}$$

Maximizing the mutual information $\mathbb{I}(X; \Delta X + Z)$ both over the scaling of the constellation points and the input distribution requires a relatively high amount of power. Instead, as shown in [Bö18], section 5.3, we will use a sub-optimal input distribution which follows from maximizing the input entropy.
We expand the mutual information as

$$\mathbb{I}(X, \Delta X + Z) = \mathbb{H}(X) - \mathbb{H}(X|\Delta X + Z) \tag{2.37}$$

and fixing Δ, we select the input distribution P_{X_Δ} that maximizes the input entropy

under our power constraint, i.e., we choose

$$P_{X_\Delta} = \underset{P_X:\mathbb{E}[(\Delta X)^2]\leq P}{\arg\max} \mathbb{H}(X). \tag{2.38}$$

Without the discrete constraint, the solution would be a Gaussian distribution. For this reason we explore sampled Gaussian distributions, also known as Maxwell-Boltzmann (MB) distributions. For each $\mathcal{X} = \{\pm 1, \pm 3, \ldots, (M-1)\}$, define

$$P_{X_v}(x_i) = A_\nu e^{-\nu {x_i}^2}, \; A_\nu = \frac{1}{\sum_{i=1}^{M} e^{-\nu {x_i}^2}} \tag{2.39}$$

We now show that P_{X_Δ} is given by

$$P_{X_\Delta}(x_i) = P_{X_\nu}(x_i) \text{ with } \nu : \mathbb{E}[(\Delta X_\nu)^2] = P \tag{2.40}$$

Proof. Consider the finite set $\mathcal{X} = x_1, x_2, \ldots, x_n$. Let f be a function that assigns to each $x_i \in \mathcal{X}$ a positive cost $f(x_i) > 0$. Define the MB distribution

$$P_{X_v}(x_i) = A_\nu e^{-\nu f(x_i)}, \; A_\nu = \frac{1}{\sum_{i=1}^{M} e^{-\nu f(x_i)}} \tag{2.41}$$

Let P_X be some distribution on $\mathcal{X}$ with $\mathbb{E}[f(X)] = P$. Choose $\nu : \mathbb{E}[f(X_\nu)] = P$

$$\begin{aligned}
0 &\leq \mathbb{D}(P_X \| P_{X_\nu}) && (2.42)\\
&= \sum_{x \in \text{Support}(P_{X_\nu})} P_X \log\left(\frac{P_X(x)}{P_{X_\nu}(x)}\right) && (2.43)\\
&= -\mathbb{H}(X) - \sum_{x \in \text{Support}(P_{X_\nu})} P_X(x) \log(P_{X_\nu}(x)) && (2.44)\\
&\overset{(*)}{=} -\mathbb{H}(X) - \sum_{x \in \text{Support}(P_{X_\nu})} P_{X_\nu}(x) \log(P_{X_\nu}(x)) && (2.45)\\
&= -\mathbb{H}(X) + \mathbb{H}(X_\nu) && (2.46)\\
\mathbb{H}(X) &\leq \mathbb{H}(X_\nu) && (2.47)
\end{aligned}$$

where the (*) marked step follows since both distributions produce the same moments for $log(P_{X_\nu}(x))$. □

2.2 Autoencoders

In the following we consider feed-forward neural networkss (FFNNs), an specific type of neural network (NN), stochastic gradient descent (SGD), and autoencoders.

2.2.1 Feed-Forward Neural Networks

FFNNs are structures which map an input vector $\mathbf{v_0} = (v_{0,1} \dots v_{0,M})$ to an output vector $\mathbf{v_k} = (v_{K,1} \dots v_{K,N})$, i.e., $\mathbf{v_K} = f_{\mathrm{NN}}(\mathbf{v_0})$. This transformation is accomplished by composing functions, which in turn are computed by layers. The number of layers, K, is commonly referred to as depth of the network. And each layer can be composed of a specific number of units (neurons), M, often referred to as width of the layer. A representation of this structure is shown in Figure 2.2

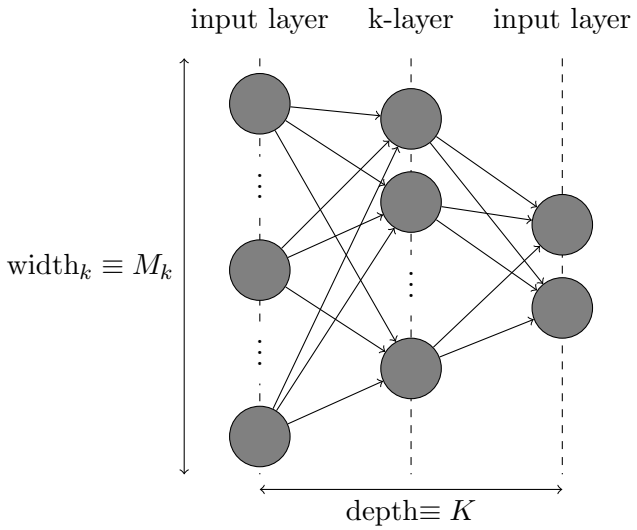

Figure 2.2: Representation of the structure of a FFNN.

Note that the width of the input and output layers must match the dimensions of the input and output vectors.
Mathematically, the output of a unit is parameterized by a weight, $\mathbf{w}_{k,m}$, and a bias, $b_{k,m}$, and can be expressed as

$$v_{k,m} = g_{\mathrm{NL},k}(\mathbf{v}_{k-1}\mathbf{w}_{k,m}^{\top} + b_{k,m}), \qquad k = 1, \dots, K \qquad m = 1, \dots, M. \tag{2.48}$$

Where in (2.48), k indicates the layer index, m indicates the unit index, and $g_{\mathrm{NL},k}(\cdot)$ is a nonlinear function, e.g., rectified linear unit, applied between layers.

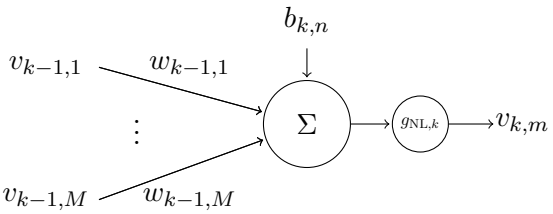

Figure 2.3: Diagram for the output's computation of a single unit as (2.48).

Indeed, without the nonlinear function the FFNN lacks the expressive power required to approximate any function [HSW89].
Finally, using matrix notation we can express the output of each layer as

$$\mathbf{v_k} = g_{\mathrm{NL},k}(\mathbf{W}_k \mathbf{v}_{k-1} + \mathbf{b}_k), \qquad k = 1, \ldots, K. \tag{2.49}$$

These structures, together with a training algorithm, help us to find parameters $\mathbf{W_k}$ and $\mathbf{b_k}$ such that $f_{\mathrm{NN}}(\mathbf{v_0})$ approximates an unknown function. To this end, the algorithm receives training sets of observed pairs of the unknown function, where each pair has the form {input, output}.

2.2.2 Stochastic Gradient Descent

To find fitting sets of parameters $\{\mathbf{W_k}, \mathbf{b_k}\}$ we define a loss function, $L(\mathbf{W_k}, \mathbf{b_k})$, that compares the current output of the NN with the desired output from the training set. The most used algorithm is stochastic gradient descent (SGD) which starts with a random set of initial values and then updates any trainable parameter, θ, with each iteration as

$$\theta_{new} = \theta_{old} + \epsilon \boldsymbol{\nabla} L(\theta_{old}) \tag{2.50}$$

where, $\boldsymbol{\nabla}$ is the gradient, and ϵ stands for the learning rate. To compute the gradient efficiently a computational graph stores the transformations to the factors which influenced the loss function.

2.2.3 Autoencoders

Autoencoders have been very successful in fields like information compression, dimensionality reduction or computer vision. In the context of ML and communication systems it was pioneered by O'Shea and Hoydis [OH17]. The idea behind an autoencoder is to transmit a particular representation of the input data so that at the output, it can be reconstructed with minimal error. This means that the desired representations must be

robust with respect to the channel impairments (i.e. noise, fading, distortion, etc.), referred to as the *bottleneck* in the autoencoder jargon. To find such representations and the corresponding mappings, $\mathbf{x}$ to $\mathbf{y}$, we make use of two FFNNs: the encoder, performing $f(\mathbf{x})$, and the decoder, performing $g(\mathbf{y})$.

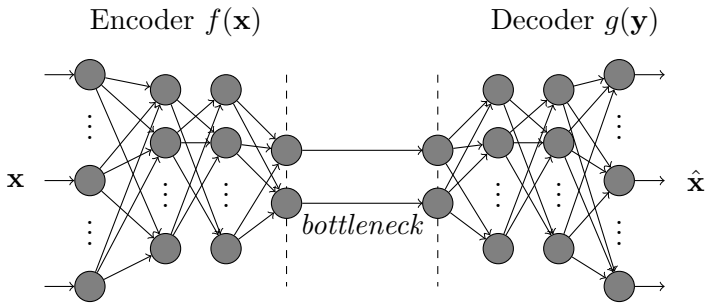

Figure 2.4: Representation of the NNs of an autoencoder.

One particular requirement for using SGD in autoencoders is that the loss gradient needs to be backpropagated all the way through receiver and channel to the transmitter. Otherwise, the transmitter parameters cannot be updated. This in turn means, that the end-to-end path must be available as differentiable functions during training.

2.3 Outlook

We can now set up the problem which we would like to address in this work. Namely, to train a NN-based autoencoder system which can find the optimal distribution and location of the to-be-transmitted constellation. By maximizing the MI during training, the output distribution must satisfy (2.18), and thus, approach the channel capacity without the mentioned penalties. Because NNs are universal function approximators [HSW89], this technique is paramount for finding the appropriate parameters over channels with a very complex, or even mathematically intractable, model.

3 Contribution

3.1 Notation

In the following we will use the notation:

$$\mathbb{I}(X, Y; D, P_M, C_M)$$

which expresses the mutual information between X and Y and D, P_M, C_M, separated by a semi-colon, are the trainable parameters of the system. D stands for the posterior probability distribution learnt by the demapper, P_M stands for the source's probability distribution learnt by the encoder, and C_M stands for the spatial distribution of the constellation points learnt by the mapper. These parameters can be seen as additional input to a function.

3.2 First implementation

In this section we break-down the autoencoder system presented by Stark *et al.* [SAAH19].

3.2.1 Optimization of trainable parameters

As we have seen in Chapter 2, the goal of probabilistic constellation shaping is to maximize the MI. To this end, defining an appropriate loss function is critical. Starting from the demodulator, the categorical cross entropy loss

$$L(D, P_M, C_M) \triangleq \mathbb{X}(P_{X|Y}||Q_{X|Y}; D) = \mathbb{E}\left[-\log_2(Q(X|Y; D))\right] \tag{3.1}$$

is appropriate for training D and C_M, but not for P_M. Training using (3.1) would have the unwanted effect of minimizing the source entropy. Consequently a modification of this loss function is necessary to ensure that the end-to-end MI is maximized. The following expansions will come handy

$$\mathbb{H}(X) = \mathbb{X}(P_X||Q_X) - \mathbb{D}(P_X||Q_X) \tag{3.2}$$

$$\mathbb{H}(X|Y=y) = \mathbb{X}(P_{X|y}||Q_{X|y}|Y=y) - \mathbb{D}(P_{X|y}||Q_{X|y}|Y=y) \tag{3.3}$$

$$\mathbb{H}(X|Y) = \mathbb{E}_y\left[\mathbb{X}(P_{X|y}||Q_{X|y}|Y=y)\right] - \mathbb{E}_y\left[\mathbb{D}(P_{X|y}||Q_{X|y}|Y=y)\right]. \tag{3.4}$$

Using the last expansion we can rewrite the mutual information in terms of the categorical cross entropy

$$\mathbb{I}(X,Y) = \mathbb{H}(X) - \mathbb{X}(P_{X|Y}||Q_{X|Y}) + \mathbb{D}(P_{X|Y}||Q_{X|Y}). \tag{3.5}$$

And the categorical cross entropy loss function becomes

$$L(D, P_M, C_M) \triangleq \mathbb{H}(X) - \mathbb{I}(X,Y) + \mathbb{D}(P_{X|Y}||Q_{X|Y}). \tag{3.6}$$

Now it is clearer, that if L is minimized during training, the source entropy is also minimized, contrary to our goal. To avoid this effect, Stark *et al.* modify the loss function as

$$\hat{L}(D, P_M, C_M) \triangleq L(D, P_M, C_M) - \mathbb{H}(X). \tag{3.7}$$

With this correction the optimization problem

$$\min_{D,P_M,C_M} \hat{L}(D, P_M, C_M) = \max_{D,P_M,C_M} \{\mathbb{I}(X,Y) - \mathbb{D}(P_{X|Y}||Q_{X|Y})\} \tag{3.8}$$

maximizes the MI.

3.2.2 Autoencoder Architecture

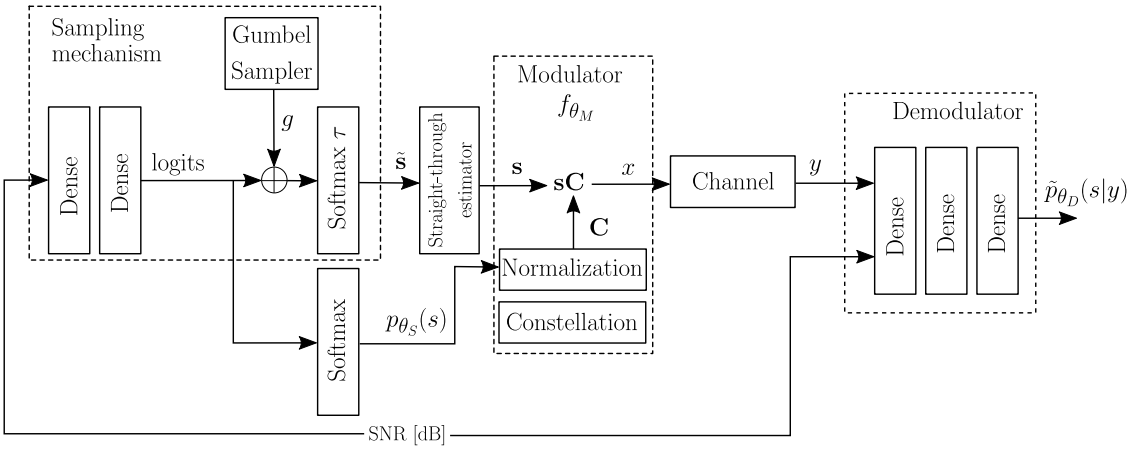

Figure 3.1: Proposed Autoencoder Architecture from [SAAH19]

Stark *et al.*'s autoencoder is made up from three major blocks: sampler, modulator, and demodulator. Figure 3.1 shows the complete architecture of the end-to-end system, where the trainable parameters $p_{\theta_S}(s), f_{\theta_M}$ and $p_{\theta_D}(s|y)$ correspond to our P_M, C_M, and D, respectively. While the modulator and demodulator blocks are similar to the proposal from [OH17], the simultaneous probabilistic shaping is possible thanks to the careful design of the sampler. By ensuring that the sampler mechanism is differentiable, the gradients with respect to each $p_i \in P_M$ are precise when calculated via SGD. In fact, the differentiability is gained by leveraging the so-called *Gumbel-Softmax trick* [JGP16], which circumvents the need for using the arg-max function to sample the discrete distribution P_M. The idea behind this trick is to replace the the non-differentiable sample from P_M, a categorical distribution, with a differentiable sample from a Gumbel-Softmax distribution, so that the gradient can be estimated during backpropagation. The generated sample vectors of dimension, M, denoted by $\tilde{\mathbf{s}}$, have components

$$\tilde{s}_i = \frac{\exp(g_i + \log(p_{\theta_M}(i))/\tau)}{\sum_{j=1}^{M} \exp(g_j + \log(p_{\theta_M}(j))/\tau)}, \qquad i = 1, \ldots, M; \tag{3.9}$$

and τ is a parameter called *temperature* which controls the degree of approximation to the categorical distribution.

We have implemented the end-to-end system using PyTorch [PGM+19]. The sampler is made out of 2 layers. The first layer is made out of 128 units with ReLU activation, and the second layer of M units with linear activations. In the forward pass, the logit output

is then processed through the Gumbel-Softmax trick and then through the straight-through estimator to produce the one-hot-encoded training set. While in the backward pass, the straight-through estimator uses the approximate one-hot vector —the output of the Gumbel-Softmax block. The trainable parameter of the sampler, P_M, is initialized to a uniform distribution. The modulator is made out of a single linear layer of N units followed by a normalization operation to ensure that the energy constraint of the constellation is maintained, i.e.,

$$\sum_{p_i \in P_M} p_i |x_i|^2. \tag{3.10}$$

If only probabilistic shaping is applied, the constellation remains fixed, e.g., M-ASK, is used. On the contrary, when geometric shaping is performed, the parameter C_M corresponds to the unnormalized constellation points. Finally, the demodulator is made out of 3 layers. The first two layers are made out of 128 units with ReLU activations, and the third layer of M units with linear activation. The trainable parameter of the demodulator, D corresponds to the *a posteriori* probabilities $p(x|y)$.

3.2.3 Autoencoder Performance

Training over the AWGN channel was performed with the Adam optimizer and the hyper-parameters of the training were: learning-rate 0.001, batch-size 10000, and number of epochs 4000. Moreover, the temperature used for the Gumble-Softmax sampler was 10. The resulting M-ASK constellations for both only probabilistic and joint probabilistic and geometric shaping are presented in Figure 3.3. Moreover the respective achieved MI for the corresponding M-QAM scheme, i.e., 64-QAM, are available for SNR values ranging from 5dB to 22dB in Figure 3.4. The results approximate the performance of the MB, which maximize the MI for the AWGN channel. From this we can infer that the learned distribution converges to the optimum.

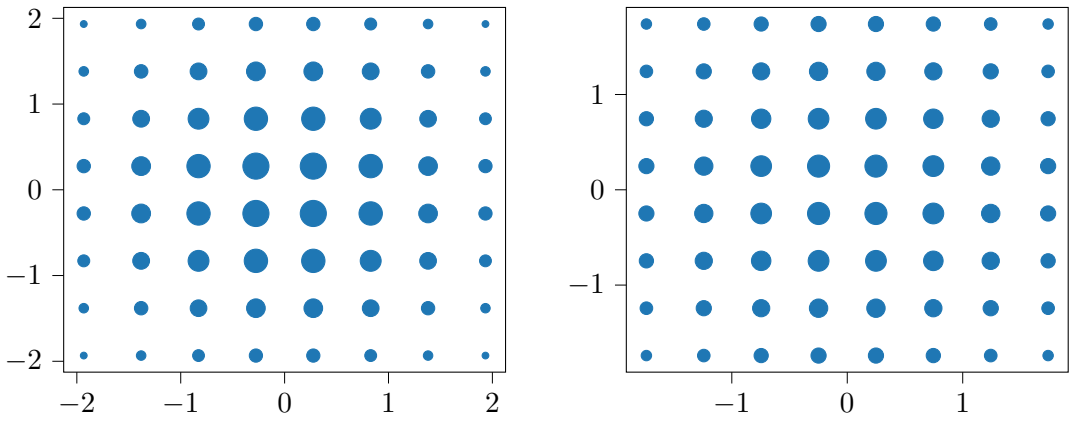

(a) 5dB (b) 18dB

Figure 3.2: Learnt probabilistic constellation shaping for M = 64. The size of the markers is proportional to the transmission probability of the symbol. When trained under 5dB, the probabilistic shaping approaches a Gaussian. While under 18dB it approaches a uniform distribution.

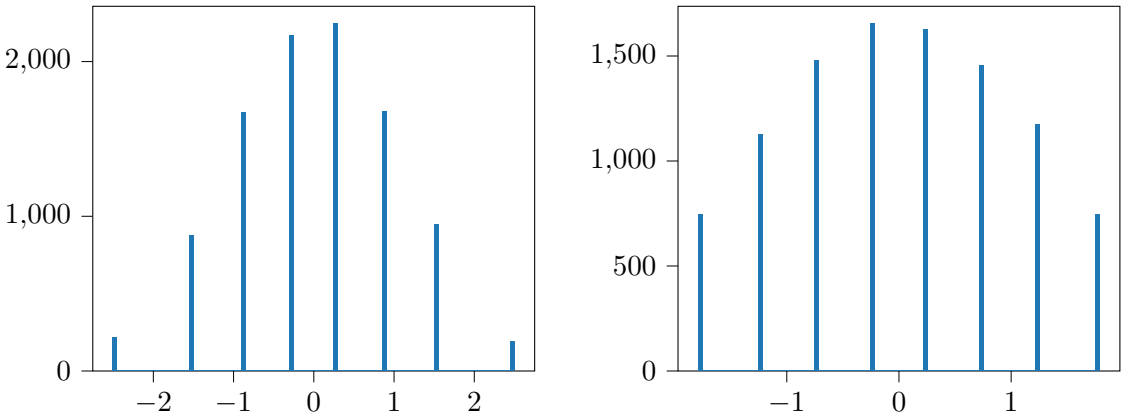

(a) SNR = 5dB (b) SNR = 18dB

Figure 3.3: Learnt joint geometric and probabilistic ASK constellations for M=8.

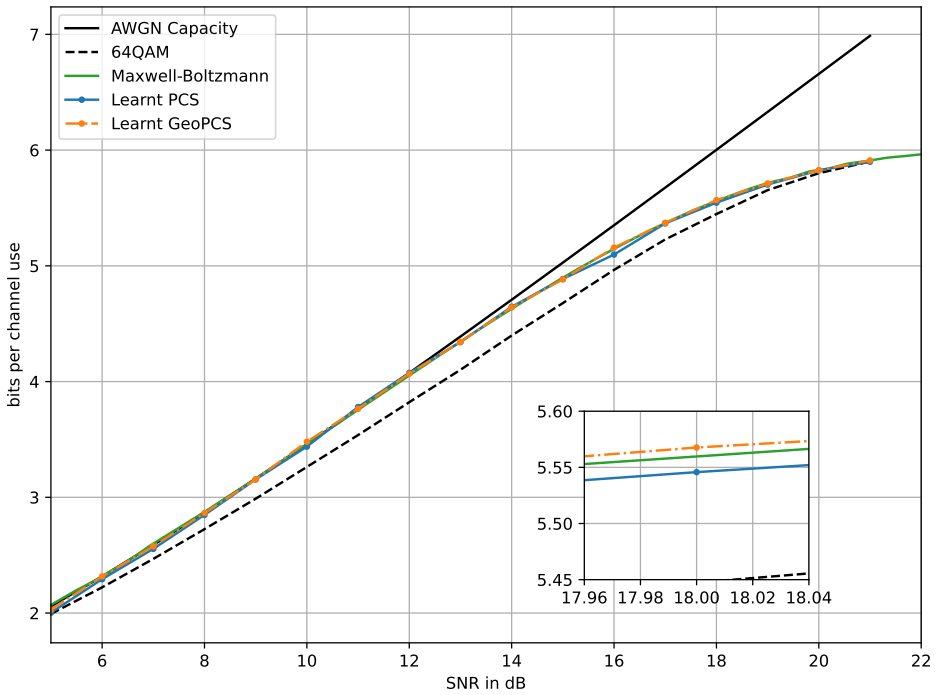

Figure 3.4: Mutual information learned by the PCS and GeoPCS for constellation size M=64 on the AWGN channel. Zoom is for the 18dB point.

3.3 Second implementation

In this section we break-down the autoencoder system presented by Aref and Chagnon [AC21]. This novel approach calls to remove the risk of numerical instabilities present in [SAAH19]. Such instabilities are introduced by the Gumbel-Softmax trick, required to make the sampler differentiable, and the sensitive extra hyper-parameters. The outstanding feature of this autoencoder is the ability to sample from the constellation probabilities without any approximation.

3.3.1 Optimization of trainable parameters

Aref and Chagnon start from the achievable transmission rate, $\mathbb{R}_{ps}(D)$, proposed by Böcherer [Bö17]

$$\max_{D,P_M,C_M} \mathbb{R}_{ps}\left(X,Y;D,P_M,C_M\right) = \max_{D,P_M,C_M} \left\{\mathbb{H}(X) - \mathbb{X}(P_{X|Y}\|Q_{X|Y};D,P_M,C_M)\right\} \tag{3.11}$$

where the entropy is maximized when the symbols' probabilities follow a MB distribution; and the cross-equivocation is minimum when $Q_{X|Y} = P_{X|Y}$. Note that when the cross-equivocation is minimum

$$\mathbb{R}_{ps}|_{Q_{X|Y}=P_{X|Y}} = \mathbb{H}(X) - \mathbb{H}(X|Y) = \mathbb{I}(X;Y) \tag{3.12}$$

the achievable transmission rates becomes the channel's MI. Typically, the gradient descent (or ascent, as we intent to maximize) allows us to solve the optimization problem by adjusting the trainable parameters as:

$$\theta_{new} = \theta_{old} + \epsilon \frac{\partial}{\partial \theta_{old}} \mathbb{R}_{ps}\left(X,Y;\theta_{old}\right) \tag{3.13}$$

for all trainable parameters $\theta \in P_M, C_M, D$. And the MI can be numerically approximated by

$$\mathbb{R}_{ps}\left(X,Y\right) \approx \mathbb{R}_{ps}\left(X,Y\right)_{\text{num}} = \frac{1}{B}\sum_{i=1}^{B} -\log_2(P(x_i)) + \log_2(Q_{X|Y}(x_i|y_i)) \tag{3.14}$$

$$= \frac{1}{B}\sum_{i=1}^{B} L(x_i,y_i). \tag{3.15}$$

Next, the following approximation usually allows to adjust the trainable parameters:

$$\frac{\partial}{\partial\theta}\mathbb{R}_{ps}\left(X,Y;\theta\right) \approx \frac{\partial}{\partial\theta}\mathbb{R}_{ps}\left(X,Y;\theta\right)_{\text{num}} = \frac{1}{B}\sum_{i=1}^{B}\frac{\partial}{\partial\theta}L(x_i,y_i). \tag{3.16}$$

However, Aref claims that although this is true for the constellation locations ($\theta \in C_M$) and the demapper parameters ($\theta \in D$), it does not hold for the constellation probabilities $\{p_1, p_2, \ldots, p_M\} = P_M$

$$\frac{\partial}{\partial p_j}\mathbb{I}\left(X,Y;P_M\right) \not\approx \frac{1}{B}\sum_{i=1}^{B}\frac{\partial}{\partial p_j}L(x_i,y_i) \tag{3.17}$$

as $\{p_1, p_2, \ldots, p_M\}$ changes the statistics of the training set.

For this reason, (3.17) must be computed differently. On the one hand, to compute the derivative of the cross-equivocation, the following expansions are useful

$$\mathbb{X}\left(P_{X|Y}\|Q_{X|Y}|Y=b\right) = \sum_{a\in Supp(P_{X|Y}(\cdot|b))} P_{X|Y}(a|b)\log_2(Q_{X|Y}(a|b)) \tag{3.18}$$

$$\mathbb{X}\left(P_{X|Y}\|Q_{X|Y}\right) = \sum_{b\in Supp(P_Y)} P_Y(b)\mathbb{X}\left(P_{X|Y}\|Q_{X|Y}|Y=b\right) \tag{3.19}$$

as combined together and applying Bayes' theorem they yield

$$\mathbb{X}\left(P_{X|Y}\|Q_{X|Y}\right) = \sum_{(a,b)\in Supp(P_{XY})} P_X(a)P_{Y|X}(b|a)\log_2(Q_{X|Y}(a|b)). \tag{3.20}$$

And so, the derivative results

$$\frac{\partial}{\partial p_j}\mathbb{X}\left(P_{X|Y}\|Q_{X|Y}\right) = \sum_{b \text{ if } x=j} P_{Y|X}(b|j)\log_2 Q_{X|Y}(j|b) \tag{3.21}$$

$$+ \sum_{(a,b)\in Supp(P_{XY})} P_{XY}(a,b)\frac{\partial}{\partial p_j}\log_2 Q_{X|Y}(a|b) \tag{3.22}$$

which can be rewritten using the expectation operator as

$$\frac{\partial}{\partial p_j}\mathbb{X}\left(P_{X|Y}\|Q_{X|Y}\right) = \mathbb{E}_{Y|X}[\log_2 Q_{X|Y}(j|b)|X=j] \tag{3.23}$$

$$+\,\mathbb{E}_{XY}[\frac{\partial}{\partial p_j}\log_2 Q_{X|Y}(a|b)]. \tag{3.24}$$

The terms can now be numerically computed as

$$\mathbb{E}_{Y|X}[\log_2 Q_{X|Y}(j|b)|X=j] \approx \frac{1}{Bp_j}\sum_{b \text{ if } x=j}\log_2 Q_{X|Y}(j|b) \tag{3.25}$$

$$\mathbb{E}_{XY}[\frac{\partial}{\partial p_j}\log_2 Q_{X|Y}(a|b)] \approx \frac{1}{B}\sum_{(a,b)\in Supp(P_{XY})}\log_2 Q_{X|Y}(a|b). \tag{3.26}$$

On the other hand, the derivative of the entropy w.r.t. p_j is

$$\frac{\partial}{\partial p_j}\mathbb{H}(X) = \frac{\partial}{\partial p_j}\sum_{i=1}^{B} -p_i\log_2(p_i) = -\log_2(p_j) - log_2(e). \tag{3.27}$$

Now, combining (3.25), (3.26), and (3.27) the derivative of the mutual information w.r.t. p_j, (3.17), can be computed as

$$\frac{\partial}{\partial p_j}\mathbb{R}_{ps}\left(X,Y;P_M\right) \approx -\log_2(p_j) - \log_2(e) + \frac{1}{Bp_j}\sum_{b \text{ if } x=j}\log_2 Q_{X|Y}(j|b) + \frac{1}{B}\sum_{(a,b)}\log_2 Q_{X|Y}(a|b) \tag{3.28}$$

Aref now indicates that the following terms can be computed via backpropagation

$$-\log_2(p_j) + \frac{1}{Bp_j}\sum_{b \text{ if } x=j}\log_2 Q_{X|Y}(j|b) = \frac{1}{B}\sum_{i=1}^{B}\frac{\partial}{\partial p_j}L(x_i,y_i) \tag{3.29}$$

while the remaining ones must be explicitly computed and added to the gradient after backpropagating. We call this step *gradient correction* and it is due to the change of statistics in the sampled batch.

3.3.2 Autoencoder Architecture

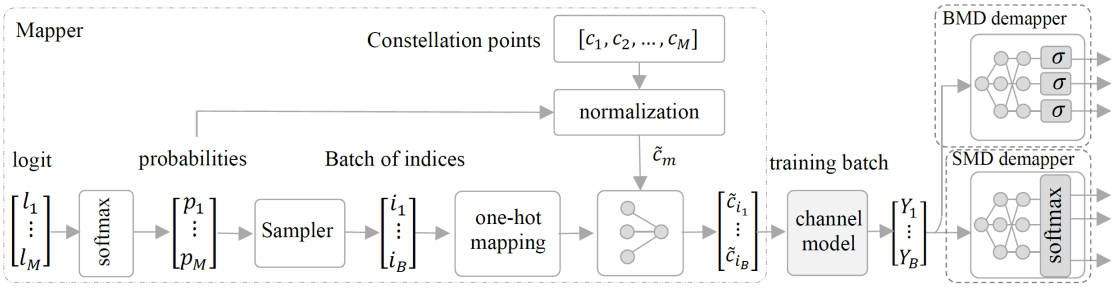

Figure 3.5: Proposed Autoencoder Architecture from [AC21]

Aref and Chagnon's autoencoder is made up from two major blocks: mapper and demapper. Fig 3.5 shows the complete architecture of the end-to-end system, where the trainable parameters are P_M, C_M, and D. Furthermore, the mapper breaks down into the sampling and the modulation mechanism. In order to sample, a single linear layer followed by a softmax layer trains the $p_i \in P_M$. Next, to produce a training symbols batch of size B, each index i is drawn about Bp_i times, for $i = 1, \ldots, M$. After, the indices are randomly permuted. Note that this sampling mechanism is not differentiable and consequently, the derivatives of the loss function w.r.t to the p_i will not be accurate. However, using the *gradient correction* factor described in Section 3.3.1, the gradient is adjusted during the backpropagation step. Similar to the previously presented architecture, the modulation mechanism is made of a single linear layer of M units and trainable parameters $c_i \in C_M$. It also includes a normalization layer to ensure that the power constraints are met. Finally, the Demapper is also made of a single linear layer followed by a softmax layer. The demapper's trainable parameter, D correspond to the *a posteriori* probability distribution $p(x|y)$ depending on the channel model.

3.3.3 Autoencoder Performance

Training over the AWGN channel was performed with the Adam optimizer and the hyper-parameters of the training are: learning-rate=0.1, batch-size=10000, and number of epochs=4000. The resulting M-ASK constellations for both only probabilistic and joint probabilistic and geometric shaping are presented in Figure 3.7. Moreover the respective achieved MI for the corresponding M-QAM scheme, i.e., 64-QAM, are available in Figure 3.8 for SNR values ranging from 5dB to 22dB. The results approximate the performance of the MB, which maximize the MI for the AWGN channel. From this we can infer that the learned distribution converges to the optimum.

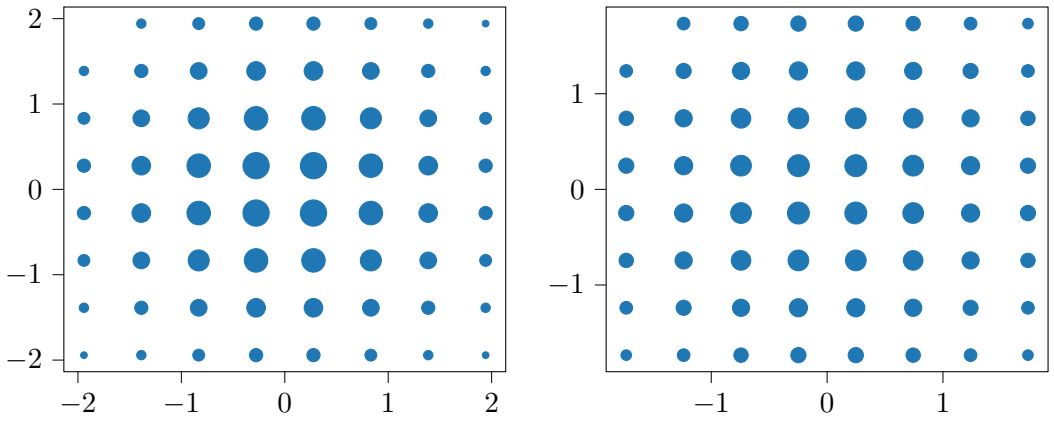

(a) SNR = 5dB (b) SNR = 18dB

Figure 3.6: Learnt probabilistic constellation shaping for M = 64. The size of the markers is proportional to the transmission probability of the symbol. When trained under 5dB, the proabapilistic shaping approaches a gaussian. While under 18dB it approaches a uniform distribution.

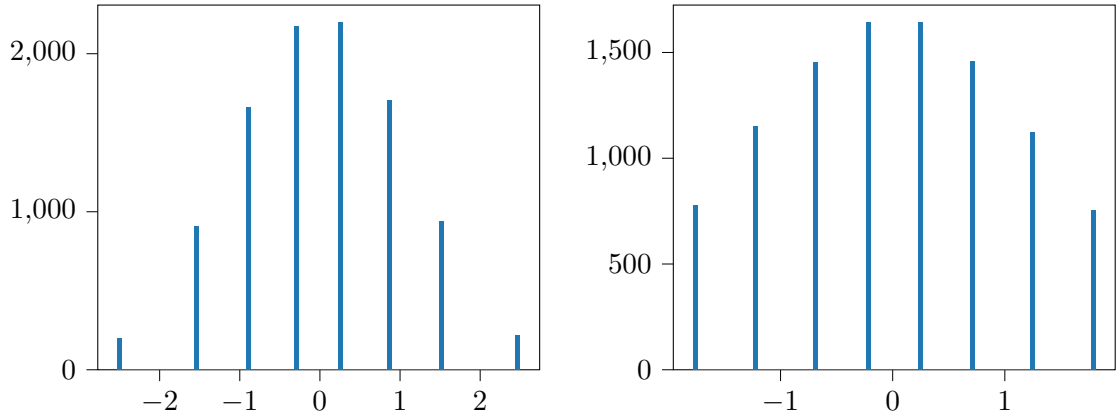

(a) SNR = 5dB (b) SNR = 18dB

Figure 3.7: Learnt joint geometric and probabilistic ASK constellations for M=8.

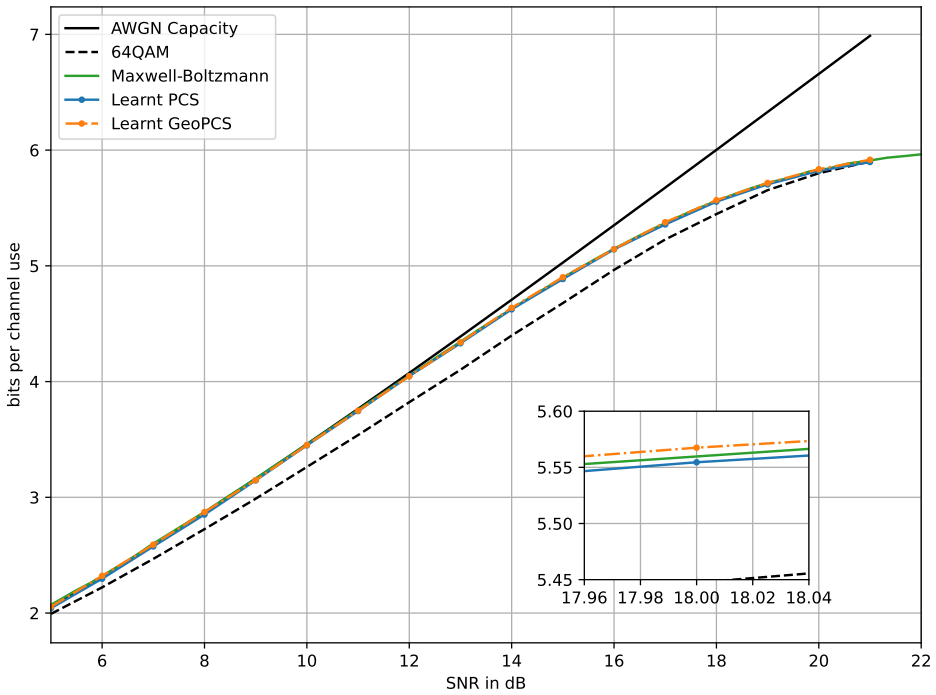

Figure 3.8: Mutual information learned by the probabilistic constellation shaping on the AWGN channel.

4 Conclusions

In the light of the above, both autoencoder proposals for joint probabilistic and geometric shaping show close-to-optimal performance over the AWGN channel. The common key for success is the choice of a loss function which would maximize the MI as well as making sure that the gradient w.r.t P_M was correctly computed. Yet, the potential of the autoencoder approach is for training over complex channels such as optical fiber. It is over these channels where we expect that different implementations will exhibit different performance. The reason for this suspicion resides in the methods for optimizing the MI. Both [AC21] and [SAAH19] introduce the entropy of the source distribution into the loss function. This in turn has the effect of adding a complementary path to the computational graph for computing the gradient w.r.t P_M without backpropagating through the channel model. Fortunately, the AWGN channel is not particularly disruptive and therefore the effect of this shortcut is minimized. However, if the channel was to introduce, for example, an interference in the form of a pilot tone, the symbols close to it should be transmitted less frequently than the non-overlapping. For this reason, we believe that [AC21] would not perform as well due to the non-differentiable sampling mechanism. Nonetheless, the Gumbel-Softmax trick does introduce numerical instabilities and further complexity, so [AC21] has also some strengths.
Finally, training over other channel models is an open research direction with some challenges but promising outcomes.

List of Abbreviations

ASK	amplitude shift keying.
AWGN	additive white gaussian noise.
FFNN	feed-forward neural networks.
MB	Maxwell-Boltzmann.
MI	mutual information.
ML	machine learning.
NN	neural network.
QAM	quadrature amplitude modulation.
SGD	stochastic gradient descent.
SNR	signal-to-noise ratio.

Bibliography

[AC21] V. Aref and M. Chagnon, *End-to-end learning of joint geometric and probabilistic constellation shaping*, 2021. DOI: 10.48550/ARXIV.2112.05050. [Online]. Available: https://arxiv.org/abs/2112.05050.

[BSS15] G. Böcherer, F. Steiner, and P. Schulte, "Bandwidth efficient and rate-matched low-density parity-check coded modulation," *IEEE Transactions on Communications*, vol. 63, no. 12, pp. 4651–4665, 2015. DOI: 10.1109/TCOMM.2015.2494016.

[Bö17] G. Böcherer, *Achievable rates for probabilistic shaping*, 2017. DOI: 10.48550/ARXIV.1707.01134. [Online]. Available: https://arxiv.org/abs/1707.01134.

[Bö18] G. Böcherer, *Principles of coded modulation. [online] available*, 2018. [Online]. Available: http://www.georg-boecherer.de/bocherer2018principles.pdf.

[HSW89] K. Hornik, M. Stinchcombe, and H. White, "Multilayer feedforward networks are universal approximators," *Neural Networks*, vol. 2, no. 5, pp. 359–366, 1989, ISSN: 0893-6080. DOI: https://doi.org/10.1016/0893-6080(89)90020-8. [Online]. Available: https://www.sciencedirect.com/science/article/pii/0893608089900208.

[JEY+18] R. T. Jones *et al.*, *Geometric constellation shaping for fiber optic communication systems via end-to-end learning*, 2018. DOI: 10.48550/ARXIV.1810.00774. [Online]. Available: https://arxiv.org/abs/1810.00774.

[JGP16] E. Jang, S. Gu, and B. Poole, *Categorical reparameterization with gumbel-softmax*, 2016. DOI: 10.48550/ARXIV.1611.01144. [Online]. Available: https://arxiv.org/abs/1611.01144.

[OH17] T. O'Shea and J. Hoydis, "An introduction to deep learning for the physical layer," *IEEE Transactions on Cognitive Communications and Networking*, vol. 3, no. 4, pp. 563–575, 2017. DOI: 10.1109/TCCN.2017.2758370.

[PGM+19] A. Paszke *et al.*, "Pytorch: An imperative style, high-performance deep learning library," in *Advances in Neural Information Processing Systems 32*, H. Wallach, H. Larochelle, A. Beygelzimer, F. d'Alché-Buc, E. Fox, and R. Garnett, Eds., Curran Associates, Inc., 2019, pp. 8024–8035. [Online]. Available: `http://papers.neurips.cc/paper/9015-pytorch-an-imperative-style-high-performance-deep-learning-library.pdf`.

[SAAH19] M. Stark, F. Ait Aoudia, and J. Hoydis, "Joint learning of geometric and probabilistic constellation shaping," in *2019 IEEE Globecom Workshops (GC Wkshps)*, 2019, pp. 1–6. DOI: `10.1109/GCWkshps45667.2019.9024567`.